Position-based dynamic of a particle system: a configurable algorithm to describe complex behaviour of continuum material starting from swarm robotics

Ramiro Dell'Erba

▶ **To cite this version:**

Ramiro Dell'Erba. Position-based dynamic of a particle system: a configurable algorithm to describe complex behaviour of continuum material starting from swarm robotics. Continuum Mechanics and Thermodynamics, 2018, 30 (5), pp.1069-1090. 10.1007/s00161-018-0663-5 . hal-01998624

HAL Id: hal-01998624
https://hal.science/hal-01998624

Submitted on 29 Jan 2019

HAL is a multi-disciplinary open access archive for the deposit and dissemination of scientific research documents, whether they are published or not. The documents may come from teaching and research institutions in France or abroad, or from public or private research centers.

L'archive ouverte pluridisciplinaire **HAL**, est destinée au dépôt et à la diffusion de documents scientifiques de niveau recherche, publiés ou non, émanant des établissements d'enseignement et de recherche français ou étrangers, des laboratoires publics ou privés.

Italian National Agency for New Technologies, Energy and Sustainable Economic Development

http://www.enea.it/en
http://robotica.casaccia.enea.it/index.php?lang=en

This paper is a pre-print. The final paper is available on:

“Position-based dynamic of a particle system: a configurable algorithm to describe complex behaviour of continuum material starting from swarm robotics“ dell’Erba, R. Continuum Mech. Thermodyn. (2018). https://doi.org/10.1007/s00161-018-0663-5

Ramiro dell'Erba

Position-based dynamic of a particle system: a configurable algorithm to describe complex behaviour of continuum material starting from swarm robotics

Abstract In a previous work, we considered a two-dimensional lattice of particles and calculated its time evolution by using an interaction law based on the spatial position of the particles themselves. The model reproduced the behaviour of deformable bodies both according to the standard Cauchy model and second gradient theory; this success led us to use this method in more complex cases. This work is intended as the natural evolution of the previous one in which we shall consider both energy aspects, coherence with the principle of Saint Venant and we start to manage a more general tool that can be adapted to different physical phenomena, supporting complex effects like lateral contraction, anisotropy or elastoplasticity.

Keywords Discrete mechanical systems · Second gradient continua · Fracture

1 Introduction

It is well-known that time evolution of a material particles system is determined by Newton's dynamics laws; however, in recent years, especially with the evolution of Computer Graphics driven by videogames applications, there has been great interest in studying the evolution of a particle system whose motion is simply determined by their relative position in a frame, without solving the differential equations of dynamics. The name of this method is position-based dynamics (PBD) [1,2]. Such methods, therefore, do not determine forces and solve differential equations but use a position-based approach. The physically based simulation of deformable solids has been an active research topic of computer graphics for many years: The aim is to simulate the behaviour of real materials to achieve graphically realistic results. In the beginning simulations for videogames applications widely used continuum mechanical methods, solving equations by finite element methods (FEM). To obtain robust simulations very small time steps are required by these methods; therefore, they cannot be used in interactive situations owing to the large machine time used.

In spite of this, still now, the first approach to simulate deformable objects by continuum mechanics is to discretize equations and to solve them using numerical integration. This can be done in several ways, but many of them are affected by the stability problem, arising from stiff differential equations and can be managed using very small time steps, resulting in high computational costs. In the meantime, Graphic Processing Units (GPU)-based solvers and adaptive meshes were growing and used to simulate complex behaviour in real time, so PBD methods became popular because they are fast, robust and easily configurable. In PBD, knowledge of traditional forces are avoided in favour of position displacements; the problem is, therefore, transformed in a geometric constraint between configurations. The final positions of the particles are determined by minimizing

Communicated by Francesco dell'Isola.

R. dell'Erba (✉)
ENEA Technical Unit Technologies for Energy and Industry – Robotics Laboratory, Rome, Italy
E-mail: ramiro.dellerba@enea.it

the distance between the reference shape and the deformed shape of a body. This minimization process requires computation of translational vectors for both shapes and of a rotation matrix. Many solutions [3,4] have been proposed to enhance the efficiency of the method that, owing to the matrix nature, can be parallelized between the cores of GPU to reduce calculation time. The PBD methods result in a physically plausible behaviour of the continuum but suffer from limitations when modelling complex material properties and describing interactions between heterogeneous bodies [5]. In our approach, we try to combine the advantages of both the continuum mechanical and the position-based approaches to describe complex physical phenomena, trying to keep the simulation easy to implement and customizable.

In previous works [6–8], we have considered a discrete particle system and have determined its evolution by a rules system that calculated the displacement of the particles, in each time step, as functions of their neighbours relative position. Since finite element method (FEM) is a reliable and well-known numerical approach for both classical and generalized continua (see [9–16] for applications), we compared the results with the corresponding classic mechanical continuum case, whose equations had been solved by FEM simulations with good agreement. In this work, we intend to generalize the concept to cover some aspects that have been left not discussed previously. The aim of the proposed model was to develop a suitable more general numerical tool capable of modelling the behaviour of deformable bodies, and to take into account higher gradient constituent relations. This approach seemed particularly promising considering the emerging role of microstructured continua, manufactured with computer-aided methods, as a technological resource (see [17–28]), because the presence of a complex microstructure often leads to macroscopic behaviours that require generalized continua for their accurate modelling (see [29–38] for more details and [39] for a historical survey on the subject). Moreover, an algorithm based on the geometric centroid of the neighbours of a given particle is consistent with the idea of (locally) minimizing an elastic potential, as the centroid has the well-known properties of minimizing the sum of the squared distances from a set of given points in an Euclidean space. Therefore, the proposed algorithm seems a natural discrete approach from the variational point of view [40–45]. The advantage of using position-based dynamics is in computational simplicity and time machine leading to results similar to those obtainable with FEM but in a much shorter time; it also provides a useful point of view that could be able to help in understanding what features are important in the deformation without solving differential equations. The general purpose of the complete work, at a future point, is to present a fast and robust method to calculate deformations of a three-dimensional body of any shape when a part of it is subject to a time-dependent displacement that supports complex physical phenomena. The approach tries to combine continuum mechanical material models with a position-based method using an explicit time integration scheme to manage complex physical effects like isotropic and anisotropic elastic behaviour as well as the effects of lateral contraction. This will be achieved without solving dynamic equations but only using a PBD method. To repeat behaviours, described by constitutive equations of the materials (e.g. Poisson effect), we introduce geometric constraint on the lattice and rules ad hoc on the displacements of the points.

We have written a complete customizable and modular algorithm easily expandable to every new feature we would like to introduce. One of the main advantages of the proposed algorithm is the fact that it automatically takes into account large deformation elasticity, which is a topic having an increasing role in today's research [46–52]. In this first paper, we are considering two-dimensional problems and two of the five Bravais lattices. In the next works, the method will be extended in order to simulate fluids and more complex structures.

2 The origin of the problem

In [53,54], the author was investigating the calculation of the geometric configuration of submarine swarm robots by the single elements; this is very important because the swarm, like school fish, adapts its configuration depending on the mission assigned. The concept of robot swarms has been a study theme, for the scientific community, for several years. Swarm research has been inspired by biological behaviours, like those of bees [55–57] for a long time to take advantage by social activities concepts [58] labour division, task cooperation and information sharing. A single-robot approach is affected by failures that may prevent the success of the whole task. On the contrary, a multi-robot approach can benefit from the parallelism of the operation and by the redundancy given by the usage of multiple agents. Moreover, the operator has the possibility to have multiple views simultaneously. In a swarm, the members operate with a common objective, sharing the job workload; the lack of one member can be easily managed by redistributing the job among the others. This feature is especially useful if we consider application as discovery and surveillance of a submarine area. A swarm can be considered as a single body, offering the advantage of a simple way of interfacing with the

human end-users and overcoming the problem of the control of a large number of individuals. In the swarm, there is no central brain, mainly because of the excess needs in band pass requested by such a brain. Instead, each individual must possess an intelligent local control system capable of managing its choices according to the choices of the neighbours on the basis of the available data. Data coherence along the swarm, being affected by the position of the member and by the data propagation speed, is also a research topic. What makes swarms interesting is their capability to fill and control large volume of water by means of a network of cooperating sensors and their capability to move in the most interesting zones, increasing density where a major need is required. The members geometrical distribution is flexible and adaptable to the task and environmental characteristics. As an example if priority is to maximize exploration volume the swarm has to maintain a great spatial dispersion and communication band pass could be slowed down; conversely, if the priority is around the risk that the amount of exchanged information becomes inadequate to ensure the correct behaviour of the multi body, the system itself can physically react by changing geometry despite of the drop in performances for the assigned task. For this reason, it is of primary importance that a single element of the swarm knows, at least locally, its configuration and can move to reach the desired one. Like birds in nature, the element of the swarm can decide its movements according to what its neighbours are doing. To this end, a positioning and control algorithm has been developed so that it reaches the desired configuration. It was then noted that a quite similar algorithm could adapt to describing PBD problems, because the movement was quite similar to deformation of a viscoelastic body. Therefore, introducing constriction generated by constitutive equations into the relationships describing relative positions between the members of the swarm, we are trying to describe the deformation of a Continuum medium. A numerical tool like this can be useful to describe complex microstructures, originated from new techniques developed, whose behaviour cannot be investigated by Cauchy Continuum theory and that are generating large quantities of experimental data. The model we are proposing can exhibit a rich range of behaviours just by changing lattice type and these relationships.

3 The algorithm

The algorithm, realized by Mathematica (Wolfram Research), to calculate deformation is based on the following steps. The two dimensional continuum body is discretized in a finite number of particles occupying, in their initial configuration, the nodes of a lattice. The kind of lattice is chosen between the five plane Bravais lattices (see Fig. 1); changing lattice we can obtain different results, all other conditions being equal. The object is discretized, see Fig. 2 as example. Four kinds of particles are considered, but the modular algorithm is opened to introduce a new kind if required to describe other behaviour; moreover, the membership category of the particles can be changed with time during body deformation. The first kind is the leaders, whose motions are assigned, i.e. the imposed strain of the body. Their motion is known and determines the motion of the other particles. The second kinds is the followers, whose motion is calculated by rules involving the motion of other particles and the characteristic of the lattice. This results in a constrained geometrical problem leading to a transformation operator between the matrices representing the particles configuration, C_t, for a discrete set of time steps $t_1, t_2, \ldots t_n \ldots$. Changing kind of lattice and interaction rules we are able to simulate the behaviour of different constitutive equations materials and reproduce different physical phenomena. By example if to determine the displacement of a particle, we consider only its first neighbours (in a chosen metric, as Chebyshev for example) we obtain a first gradient behaviour, while considering also the second shell of neighbours we obtain second gradient effects, see Fig. 3. The third kind of particles belongs to the frame. To avoid edge effects, like corners collapse, we surround the body by an external frame of point; a shell, so that any followers look to have the same boundary condition of all the others. This is because the follower position is calculated by a function of its neighbours; therefore, it is important that any follower works in the same conditions. Without the frame, a corner point has less neighbours, with respect to an internal point; so far if its coordinates are determined, as example, by barycentre of its neighbours, this point will be attracted towards the inside and the lattice and will collapse on the other points. The motion of the frame is much simple: It only follows the motion of an assigned follower of its competence; in case the assigned followers are more than one(i.e., in a corner), then an average displacement (or a more generic rule) is computed. The frame can be something more complex than a single shell; as an example if we are considering second gradient interaction, we need a double shell to reach our aim that is the homogeneity of the boundary conditions for all the followers. In Fig. 3, an example of the three kinds of points is shown, together their first neighbours in the Chebyshev distance ρ, defined in R^2 as:

$$\rho((x_1, x_2,), (y_1, y_2,)) = \mathrm{Max}(|x_1 - y_1|, |x_2 - y_2|)$$

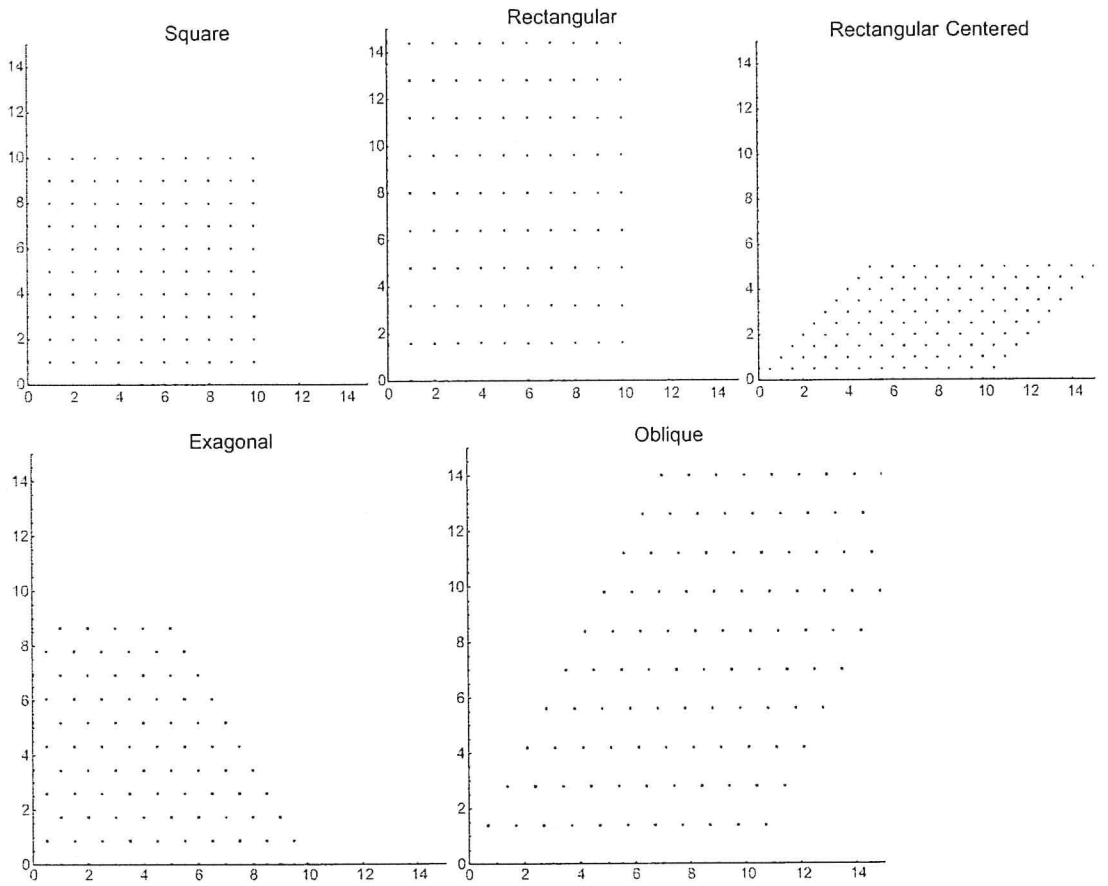

Fig. 1 Bravais plane lattice

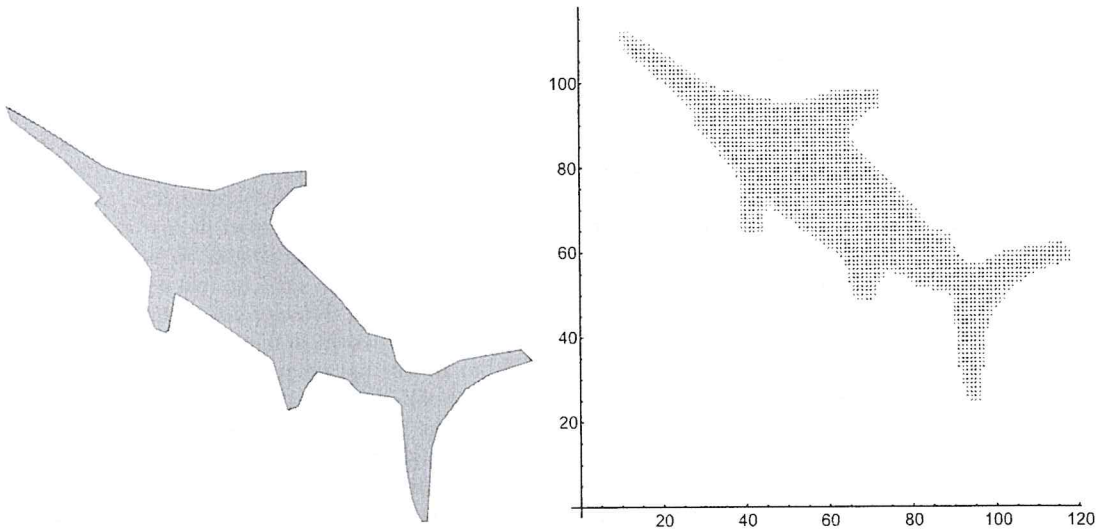

Fig. 2 Example of discretized object in the chosen lattice with frame (yellow points) (colour figure online)

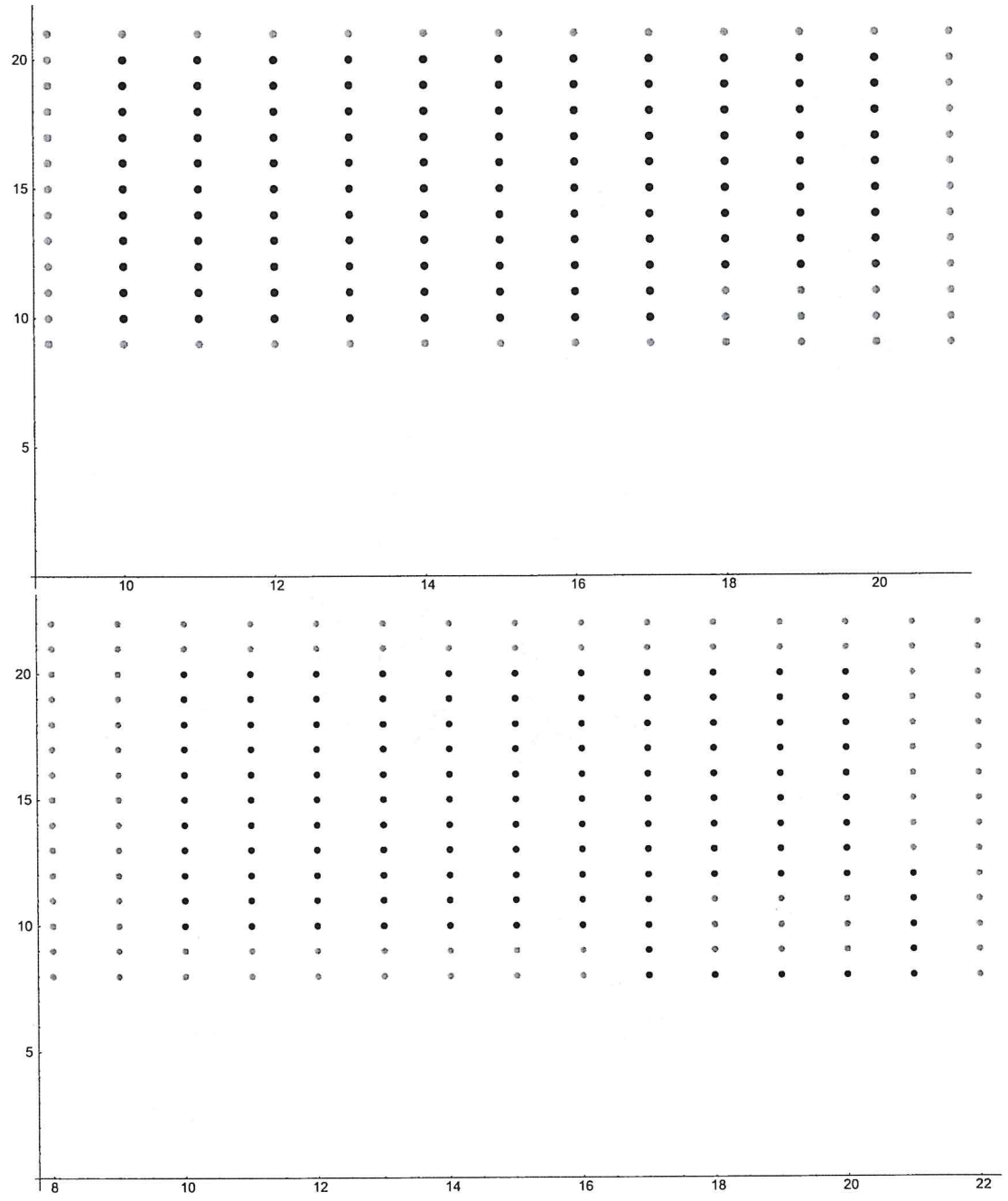

Fig. 3 Example of the three kinds of points. Leaders (red), followers (blue) frame (yellow). An example of first and second neighbours in Chebyshev distance is shown (green points and black) (colour figure online)

The last kind is the fictious. They are ghost-like points introduced in some particular case, as to manage fracture; we shall discuss them later.

The process is the following (see the flow chart in Fig. 4). We choose a two-dimensional body. Choose one of the Bravais lattice and discretize the body to obtain a discrete matrix to represent it. We now decide the constrain of the lattice and the interaction rules between the followers, in order to describe the correct behaviour of the constitutive equations of the materials. As an example, we can decide that the lattice has no

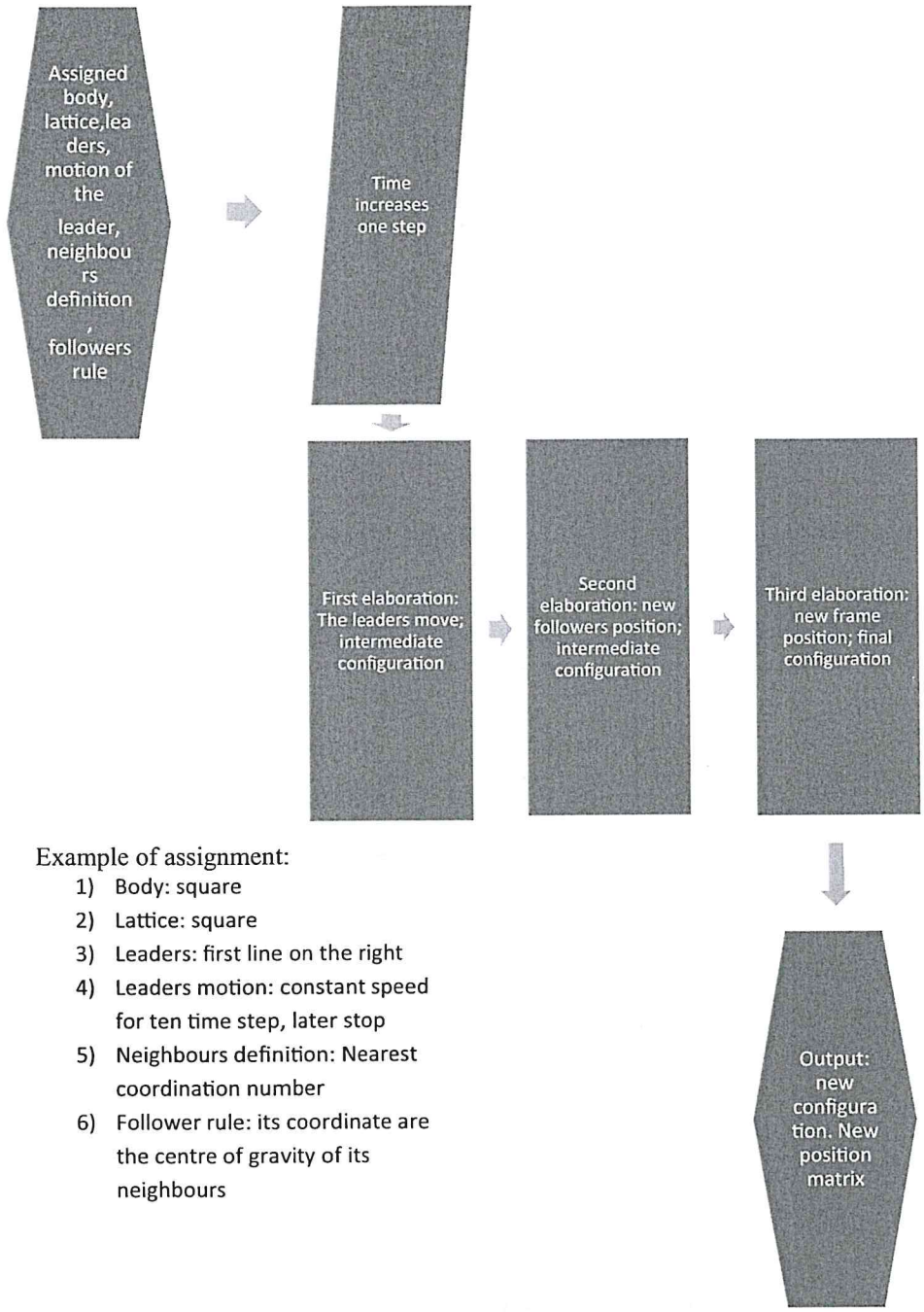

Fig. 4 Flow chart of the process

constraints and displacement of a follower point is the average value of the displacements of its first neighbours (first gradient). We build an adequate frame to avoid board effects. We decide the motions of some points, called leaders, for all the time windows we are investigating; we can also decide that they will be leader only for a certain time and late become followers (Category change).

Now we can calculate, for each time step, the new configuration of the lattice in three separate operations. When time increases from t_0 to t_1, the leaders change their position from initial configuration according to the prescribed equation. So far we build a new intermediate lattice where only the leaders have been moved.

Now we take care that the followers are no longer in equilibrium position owing to the leaders displacement. How we can calculate it? As an example, if the interactions rule establishes that a follower has to be in the barycentre of all its neighbours, we calculate the new position of each follower, taking into account the leader displacement. So far note as at this stage only the leader's neighbours are involved. Finally, we take into account the rules governing the frame displacement. This is our lattice at time t_1. It is important to note as reached the configuration is not an equilibrium one, because the three operations must be repeated for many time step, after the leaders stop. To be more clear if at time step one the leaders have moved, we calculate the followers displacement. This operation involves only the neighbours of the leaders and not the other far followers. Later, we calculate the frame displacement to close the loop. Now there are some followers (the neighbours of the leaders neighbours) that there are no longer in equilibrium because there has been the displacement of the leader's neighbours. So we need another time step to adjust the configuration and so on. At a certain time, all the followers are involved in the calculation. The followers will suffer the leaders motion after $(k-1)$ time steps where k is the distance from the leaders, measured in layers. In this meaning, the leader motion "propagates" through the lattice to influence the position of all the followers in a time depending on the lattice dimensions and how many shell of points are being considered in the neighbours definition. In the same way, when leaders stop, the followers continue to adjust their position in many time steps. We have often used the rule of centre of gravity to determine followers position that mean:

$$x_j(t) = \frac{\sum_{k=1}^{\text{all neighbours of } j} x_k(t)}{N}$$

where N is the number of neighbours. The same equation is used for the y coordinate.
But we can use different rules in order to approximate different constitutive equations, i.e. we can introduce relative distance between the points into the rule to weight their influence on the followers movement and simulate Hook law, where force is increased with increasing deformation:

$$x_j(t) = \frac{\sum_{k=1}^{\text{all neighbours of } j} \text{dis}(k, j)\, x_k(t)}{\sum_{k=1}^{\text{all neighbours of } j} \text{dis}(k, j)}$$

where dis(k, j) is the Euclidean distance between the points k and j.
Or we can mix x–y coordinates into the rules so as to make that movement in x direction has effects on the y coordinate (lateral contraction).

$$y_j(t) = K * \left(x_j(t) - x_j(t_0)\right) * \text{da} + \frac{\sum_{k=1}^{\text{all neighbours of } j} y_k(t)}{N}$$

where da is a function of the distance from the central axes, K is a parameter determining the response force, and $x(t_0)$ is the initial x coordinate. This rule leads to the Poisson effect, because we have explained it as an expansion of the x coordinate having influence on the y coordinate.
Moreover, we can force the followers movement to overcome the barycentre equilibrium position leading the lattice to oscillate. This will be done in a future paper.

Practically, we have a transformation operator between matrices representing initial and final configuration. Take into account that the algorithm is written in a way that, if you like, the neighbours can dynamically change to every time step. The choice to fix the neighbours of every particle at the initial time t_0, and to not change them during time evolution of the configurations lies in the desire to imitate a crystalline lattice and therefore to deal with solid phase materials. This means the concept of neighbours is Lagrangian, and neighbourhood is preserved during the time evolution of the system; the only exceptions arise with the fracture algorithm as we can see later. Also the definition of neighbours is customizable by changing metric; as an example, we can consider points whose Euclidean distance (weighted or not is another possibility to take into account anisotropies) is less than a threshold or, more physically, the coordination number of the lattice chosen. In the case of second gradient, we enlarge the set of points with a supplementary shell.

We also like to introduce a pseudoenergetic consideration to give a contour plot of the strain distribution; in the elastic case, we can consider the square distance between the actual configuration C and the reference configuration C_0. It must be underlined that this artifice has no direct connection with the usual energy definition (this is the reason we use the term pseudoenergy) but could be useful in understanding deformation. Therefore, we introduce two formulations PE1 and PE2 for this concept. The first is given by the value, for each step time and in each point describing the configuration, of the sum, extended to the neighbours, of square of the

difference between the distances of the point from its neighbours less the distance in the initial configuration i.e.

$$\mathrm{PE1}\,(t, j) = \sum_{k=1}^{\text{all neighbours of } j} (\mathrm{dis}\,(t, k, j) - \mathrm{dis}\,(t_0 k, j))^2$$

where dis(t, k, j) is the Euclidean distance between points k and j at time t. This is the formula for the point j at time t
The reason of this choice lies in the attempt to simulate potential energy of material points subject to Hook law. Be careful with this concept in fracture case, it considers the positions of the real points, not the fictitious, so it still needs to be work around.
To compare time contiguous configuration $C_t$and C_{t-1}, we define for each point j and each time t

$$\mathrm{PE2}\,(t, j) = ||C_t - C_{t-1}||$$

where $||$ is the Norm of the vector defined by the point j at time t and $t - 1$.

4 The algorithm in fracture case

To manage fracture phenomena, we assume the interactions are decreasing with increasing distance between particles. Therefore, when Euclidean distance between points is "great", they lose their interaction. To address the problem, we start simply considering a threshold effect between neighbour elements, so that when the distance overcomes the threshold these elements are not anymore taken into account. To preserve symmetry of the Lagrangian neighbours, we introduce ghost-like points called fictitious elements. They have the purpose of balancing the calculations of the point's displacements. Where are these ghost elements posed? Our choice is to put them in a position which is able to recover the original shape of the lattice. All the properties of these fictitious elements are the same of the followers but their motion is not considered, because they are not in the list of the followers. They are just in the right position to balance the cell. As we have seen [6], a change in their position produces effects such as the contraction or loosening of the lattice in the deformed configuration. In fact, varying the distances of the fictitious elements after fracture from the true elements, plastic-like and elastic-like behaviours can be obtained. As elastic behaviour in fracture, we mean the property of the fracture edges or of the disconnected pieces originated after fracture has occurred, to recover its original shape. The algorithm can be easily generalized to second gradient by introducing two different thresholds for the two shells of neighbours.

5 Approached types of problems

In the previous paper [6], we investigated some easy applications of a first version of the algorithm. Now we have reformulated the whole procedure, rewritten the code and in this first paper we approach some bidimensional problems of a simple shape object subject to imposed strain of some leaders which are significantly interesting to show the coherence of the model and its adaptability in showing different physical phenomena by changing some parameters. In particular, in this paper, we analyse:

(a) Simple strain and release; tensile test of rectangular shape specimen.
(b) The importance of the rules: the Poisson effect.
(c) The importance of the gradient.
(d) Simple fracture case
(e) Saint Venant principle of local action verified
(f) The importance of the lattice on different way of fracture.
(g) The importance of the rules for the frame evolution.

The features of each test can be summarized in Table 1 like this:
For every test, we shall show and discuss the movement of the particles, the XY movement of a significant particle (if present) and some pseudoenergetic considerations by PE1 or PE2.

Table 1 Description of the test

Parameter description	Value
Test description	Tensile test with relaxation
Lattice type and number of points	Square (10×10)
Step time of motion	10
Step time total	400
Neighbours concept	Coordination number of the lattice
Gradient	First
Interaction rule for followers	Position as centre of gravity of the neighbour
Use of weight distance	No
Limit distance for fracture	No fracture
Distance where the fictitious are placed	Not applicable
Leader points	First column on the left clamped. First column on the right up to time step 10; after they became followers
Leader velocity	Constant velocity in positive × direction (0.35 unit/step) for the column on the right up to time step 10, 0 later

6 Numerical results

Case (a) Simple strain and release; tensile test of rectangular shape specimen

The first numerical simulations will concern the behaviour of the system described in Table 1. We are considering a square sample undergoing strain from one side (the other side is clamped) at constant velocity in x direction (speed 1, 2 unit/step time). At a certain time, the pull is released and the leaders return to original configuration (they have changed category and are followers) attracted by the other points. So far the leaders start moving with constant velocity up to a certain time; later they became followers subjected to the rule like the other followers. The simple rule, governing followers motion is that every point must be placed in the barycentre of its neighbours; the neighbours are determined by the coordination number of the lattice; therefore, the leaders motion implies a displacement of the first layer that propagates in successive time steps. This means the displacements, at each time step, involve a larger shell of points until to regards all the lattice points. The neighbours points are determined by the coordination number of the lattice or, in second gradient, considering also the neighbours of the first neighbours. In Fig. 5, we can see the configuration of the lattice over different time together with the PE1 contour plot.

From the figure, we can outline that the x displacement of the points seems do not depend on the y coordinate; however, looking at the PE1 picture, we can note a light convexity that does mean this is not true. A deeper examination of the points displacements confirms as close to the frame the displacements, along x coordinate, are lower with respect to central points. This can be explained as an edge effect. In fact if we consider points on the same vertical lines, those that are close to the frame follow the neighbours with a little delay owing to the different rule determining the displacement of the frame and of the followers. So they see a different situation with respect to, as an example, a central point. This effect will be more evident in other computation later. Moreover, we can note as the maximum value of PE1 (red area) is not on the leader line but just on its left; this because, in this case, the leaders have in their neighbours, some points of the frame that are always close to them. This is also evident in Fig. 6 where the PE2 is shown and contiguous configurations are compared. We can avoid this convexity effect using a different frame or mirroring the followers to obtain an infinite sample. Finally, it should be noted as at $t = 401$ the lattice is not back completely to the reference configuration owing to asymptotic process of relaxation.

Now we would like to see the evolution on time of a central point of the lattice. In Fig. 7, the numbered lattice, with leaders, followers and frame are shown and in Fig. 8, the behaviour of the PE1 versus time is shown for the central point $j = 67$. Points are numbered from left to right and from bottom to up.

The value of the PE1 increases notably when points are pulled but decrease in quite a parabolic-like way when they become followers subjected only to the rules leading to equilibrium barycentre position. This has similarity with Hooke's law where the energy is proportional to the square of the displacement. If we change the point, around $j = 67$, the shape of the curve, showed in Fig. 9, remains qualitatively the same.

In Fig. 9, the evolution with time of the coordinates of central point $j = 67$ is shown. Also in this picture, we can recognize the coordinate x increases linearly (velocity is constant), after a delay, owing to the propagation time, and later decrease with parabolic like behaviour to the original position. No oscillation can be observed with this kind of rule.

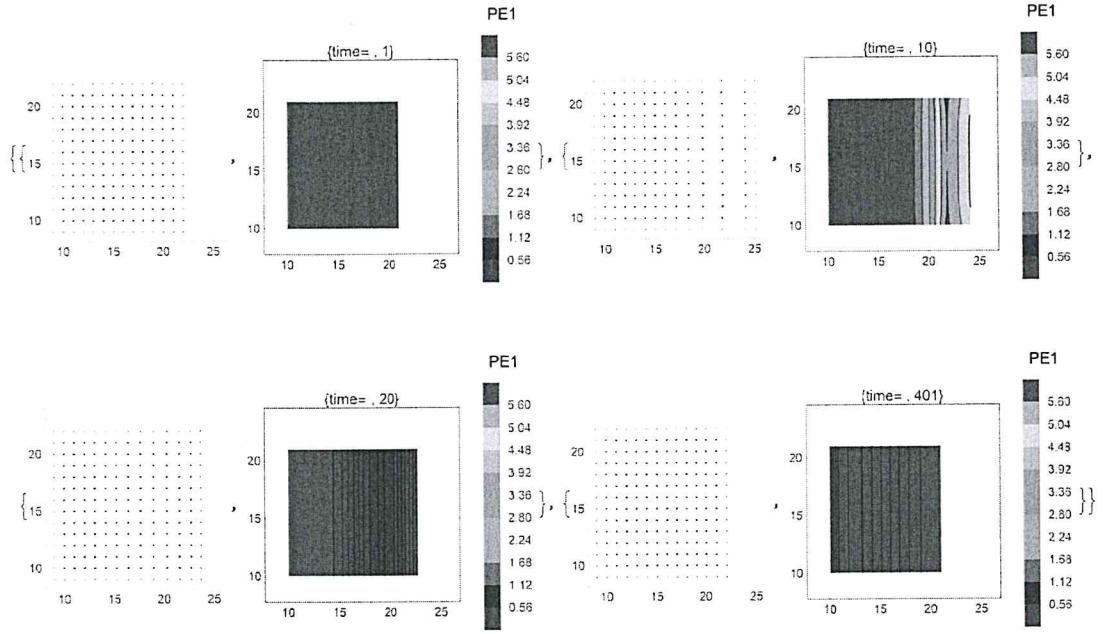

Fig. 5 Configuration of the lattice over different time (1, 10, 20 and 401) and PE1 contour plot

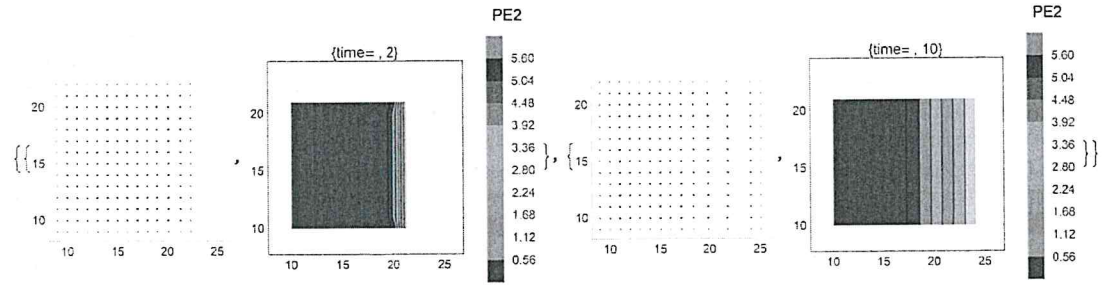

Fig. 6 Configuration of the lattice over different time (equivalent to 2 and 10 of PE1) and PE2 contour plot

Case (b) The importance of the rules: the Poisson effect
In the second case, we change the interaction rules; the case is the same as (a) (without release, the leaders stop after movement and the motion steps are 100), but the follower position is determined not only by a barycentric equation but the rule take into account the other coordinate. We call this method "mixed coordinate".
In Fig. 10, we can see the configuration of the lattice over different times together with the PE1 contour plot. Lateral contraction can be seen. Note that there is a relaxation time, because the followers need time to adapt themselves. This is due to the rules expression and can be tuned as you desired. The PE1 value seems to follow the configuration; here is more evident the edge effect leading to concavity effect towards left side.
In Fig. 11, the evolution with time of central point $j = 67$ is shown and the lateral contraction, in y coordinate, is evident. The point is above the central line so their y coordinate decreases.
Case (c) The importance of gradient
The case is the same as (b), but the follower position is determined by a second gradient neighbours.
In Fig. 12, we can see the configuration of the lattice over different times together with the PE1 contour plot. Lateral contraction can be seen in a less pronounced way; this is because if we take into account a larger number of neighbours, the effect is amortized. The Pe1 plot enhances the convexity of the first line of follower. We shall see better as, in the fracture case, second gradient has much more influence in some cases.
In Fig. 13, the evolution with time of the central point $j = 67$ is shown and a lower lateral contraction, with respect the first gradient case, can be outlined and its evolution with time is quite different.
Case (d) Simple fracture case

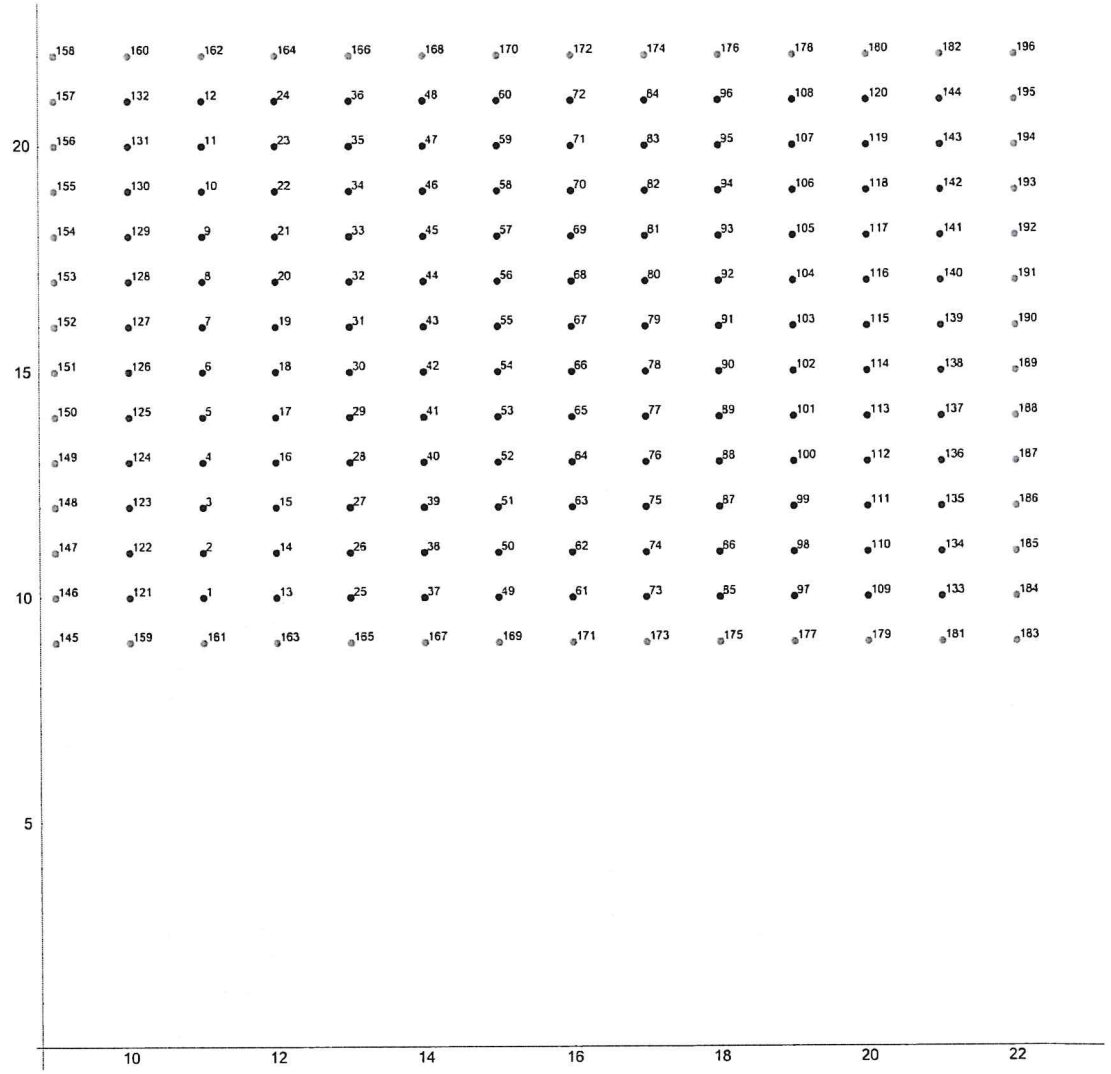

Fig. 7 Numbered lattice. Red points are the leaders, yellow the frame and blue the followers (colour figure online)

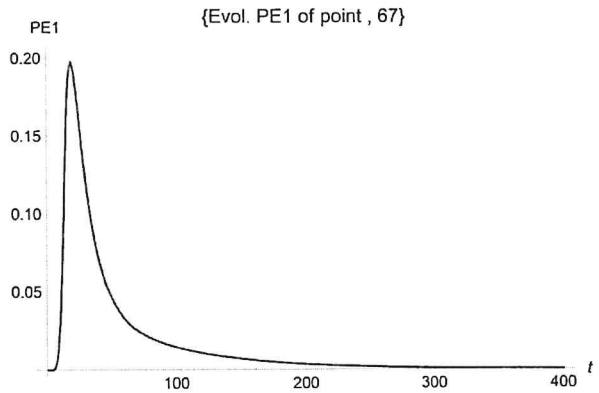

Fig. 8 PE1 versus time

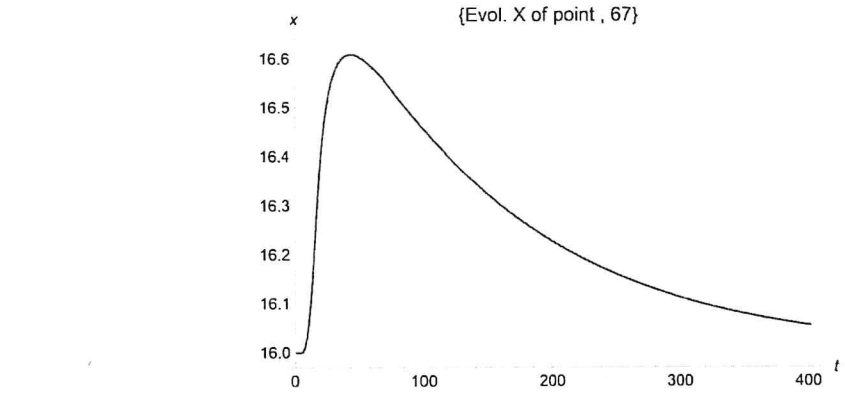

Fig. 9 Evolution of the central point's $j = 67$ versus time

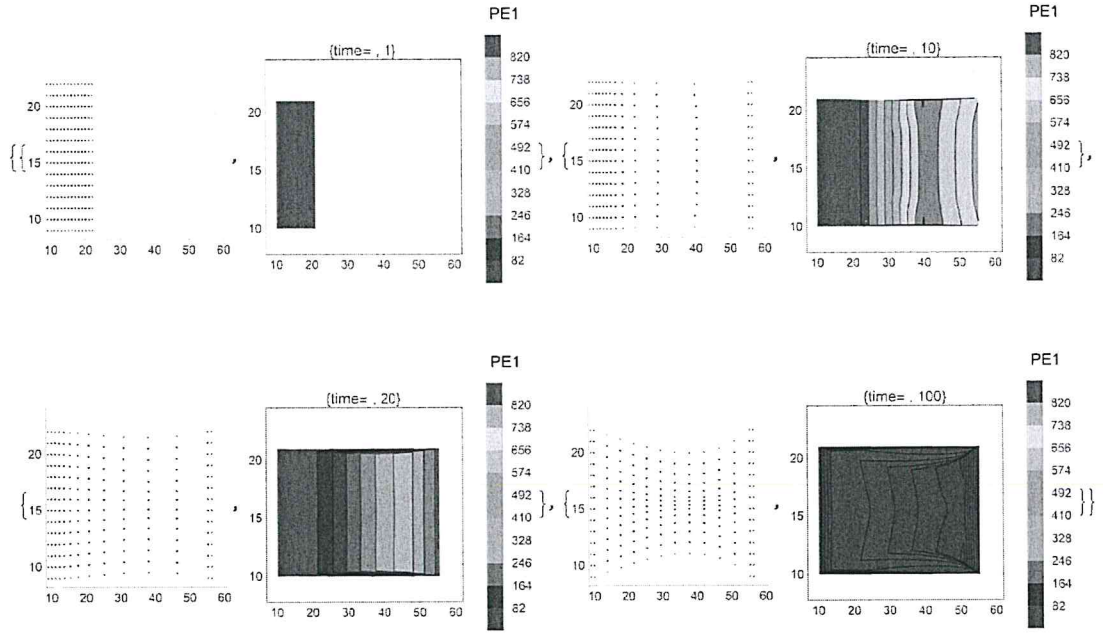

Fig. 10 Configuration of the lattice over different time (1, 10, 20 and 100) and PE1 contour plot

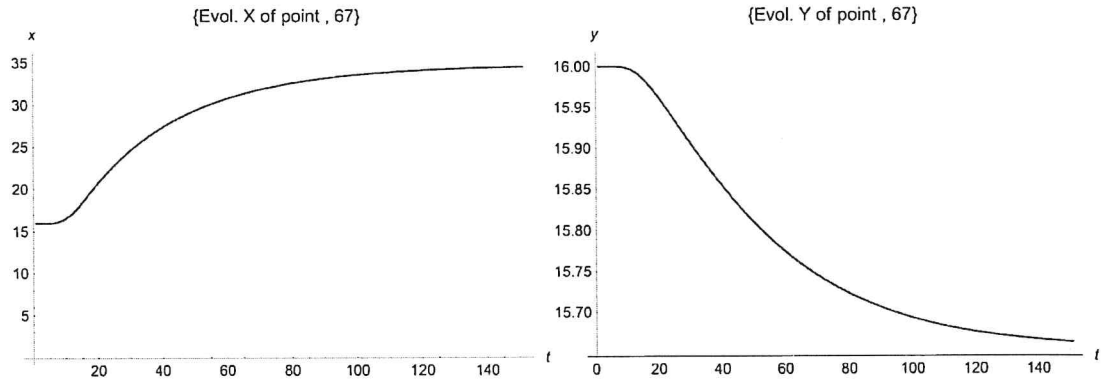

Fig. 11 Evolution of the central point $j = 67$ versus time

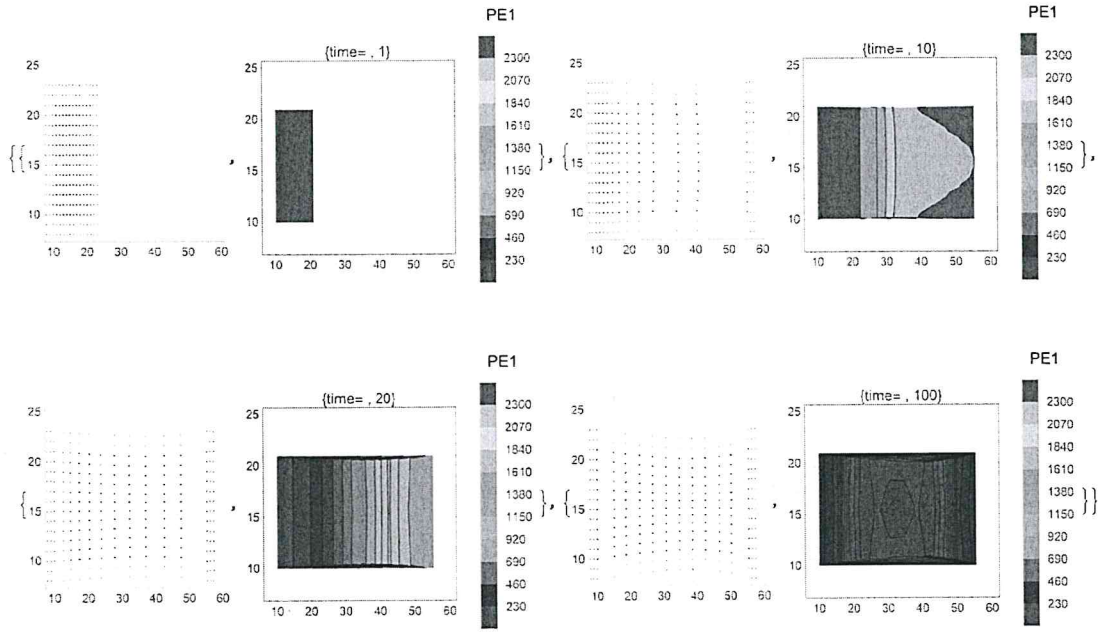

Fig. 12 Configuration of the lattice over different time (1, 10, 20 and 100) and PE1 contour plot. Second gradient

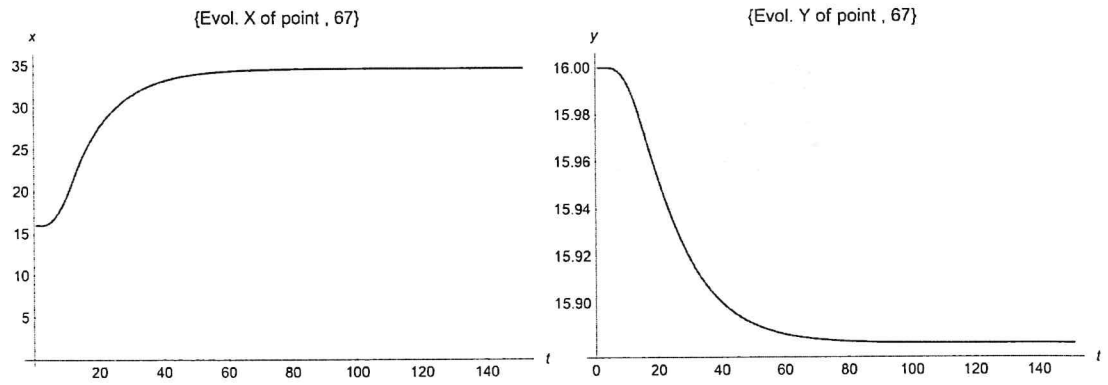

Fig. 13 Evolution of the central point $j = 67$ versus time

A simple fracture case can investigate with the same parameter of the preceding but with the rule for follower to be in the centre of gravity of its neighbours (no Poisson case). Choosing a distance fracture of about 10 units in the following pictures, we can see that the vertical fracture line is different in the case of first (see Fig. 14) or second gradient (see Fig. 15). Points close to the frame are detached before the others from the leaders, and this effect is more marked in second gradient case. This can be explained with the different neighbours number and also with the larger influence of the frame with respect to the first gradient case.

Remember that in the fracture case the pseudoenergy plot is less indicative, because we are calculating it using distance between points greater than the fracture threshold. In a future work, we will consider a better definition of this parameter.

The importance of second gradient can be outlined in Fig. 16 where x coordinate evolution versus time of x coordinate of point 103 is showed. The point is situated in middle value as y coordinate and two lines on the left of the leaders line; differently from first gradient mode, a complex behaviour can be observed because after the fracture, the x coordinate has a sort of rebound. This can be explained as follow. After the fracture, the point tries to return its initial position (on the left), but later some fast point on its right tries to deviate it

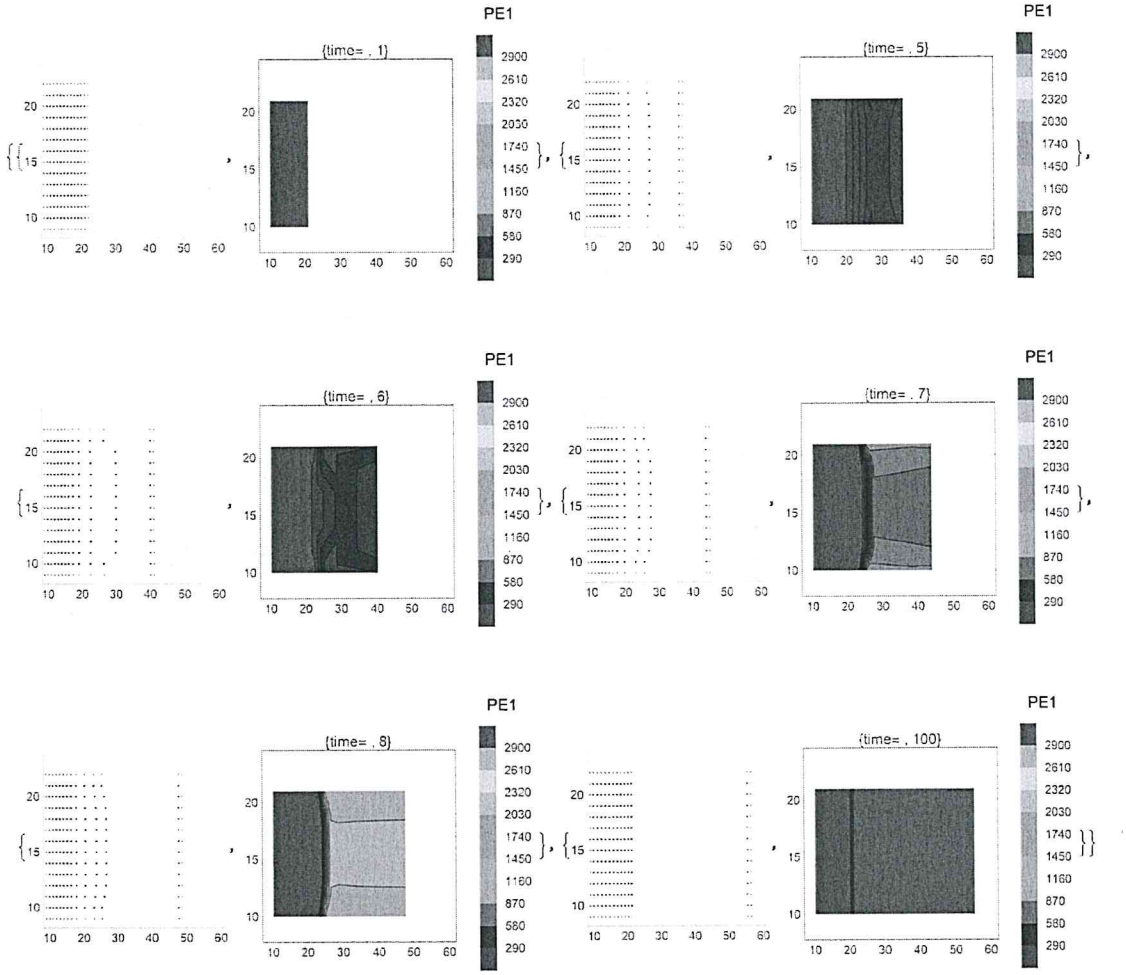

Fig. 14 Configuration of the lattice over different time (1, 5, 6, 7 and 100) and PE1 contour plot, fracture in tensile test. First gradient

to the right. When the group is compacted, they go back all together to initial configuration. So far, change in the parameters can lead to complex evolution behaviour of the lattice

Case (e) Saint Venant respect

In this case, we shall verify the local action principle, whereby the tension at one point is not influenced by the motion of the external particles to an arbitrarily small circle of the particle in question. To this aim, we consider four internal points that diverge from their initial configuration; practically, we choose four internal points as leaders with opposite movement along the bisectors of the corners.

In Fig. 17, we can see the configuration of the lattice in different time together with the PE1 and PE2 contour plot.

As can be seen, remote particles are not interested in what is going on close to the leaders.

Case (f) The importance of the lattice on different ways of fracture.

The fracture mechanism is strongly dependent on lattice characteristics. In the next case, we choose a hexagonal lattice, instead of square; the coordination number, i.e. the number of neighbours is also changed, being a characteristic of the lattice. In Fig. 18, we are considering the fracture case for the hexagonal lattice (all parameters are the same as the square lattice fracture case). The behaviour is very different from the square lattice case as we expected. It can be noted that a point of the frame remains in the middle of the displacement. This can be explained as follows. The rules regarding the frame are simple; each point of the frame is linked to an assigned follower and its displacement from time t to $t+1$ is the copy of the follower. However, in some cases, the followers assigned to one point of the frame could be more than one. In such cases, we can choose

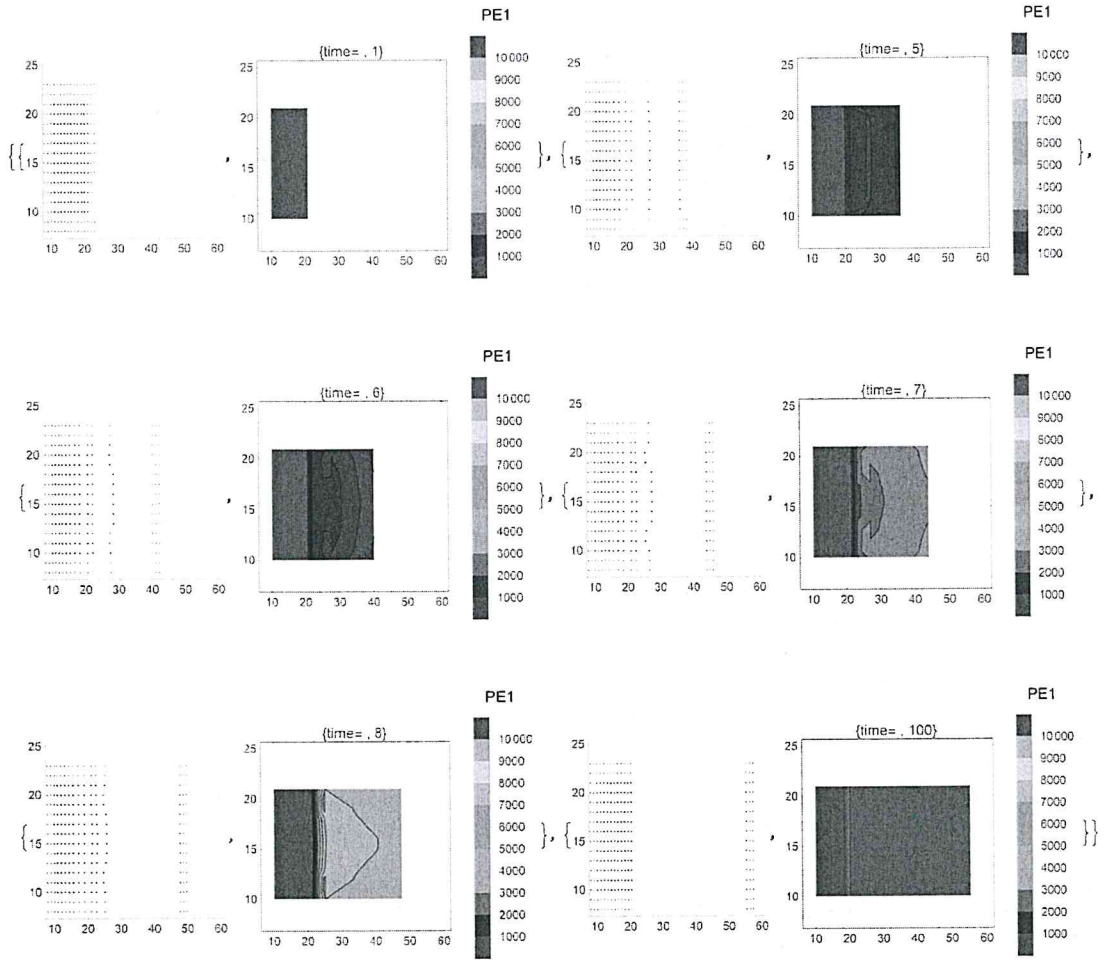

Fig. 15 Configuration of the lattice over different time (1, 5, 6, 7, 8 and 100) and PE1 contour plot, fracture in tensile test. Second gradient

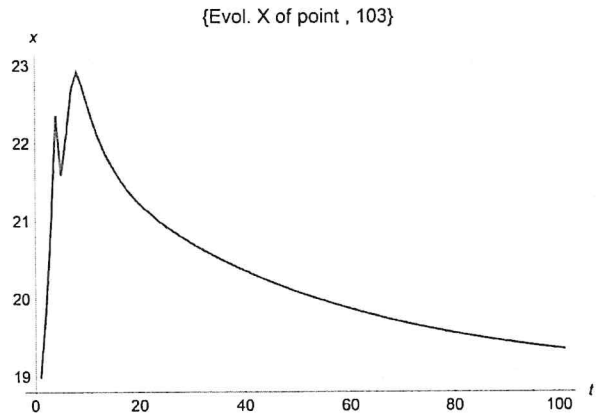

Fig. 16 Evolution of the second follower line point $j = 103$ versus time

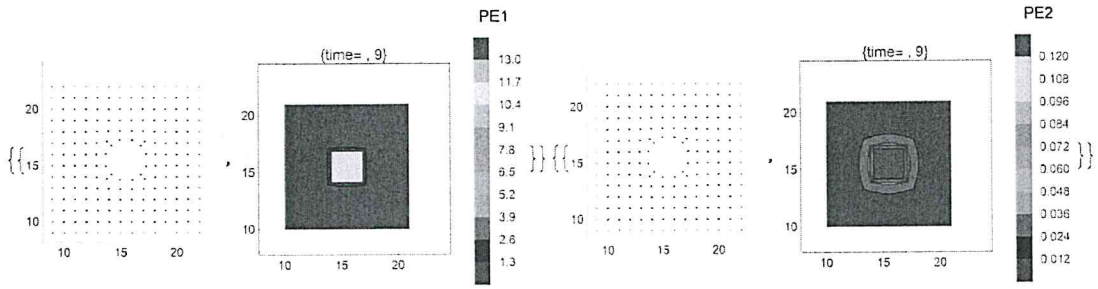

Fig. 17 Configuration of the lattice at time (9) with PE1 and PE2 contour plot

to take one of them or to consider the displacement of the point as the average value of the displacements of all its followers linked to it. This is the reason that two points of the frame remain in the middle: they are stressed from two opposite sides. Look at Case (g) for a different frame rule. The behaviour is very interesting; it can be noted that a different equilibrium configuration is reached because the frame is changed and the fictious are not in the list of the followers. In the case of Fig. 18, this results in a concave final surface, owing to the modified frame.

A rebound mechanism can be outlined from Fig. 19 This is typical of a hexagonal lattice; you can see that in the square lattice this behaviour does not exist.

Also in this case second gradient mode attenuates the effects, see Fig. 20. No rebound (Fig. 21) can be outlined and the equilibrium configuration, after the fracture is similar to the original. Cuspidal point in x coordinate, after about 100 step, can be attributed to a second fracture happening.

Case (g) The importance of the rules regarding frame motion.

We have just noted that for the hexagonal lattice there were two frame points that remain in the middle. To stress the importance of the rules also for the frame now, we are considering the same case (see in Fig. 22) where only the first of the followers are linked to each point of the frame. The behaviour is completely different and more similar to the square lattice.

Also the convexity of the surface fracture is changed with respect to the preceding case (second gradient with average value for the frame) being similar to the square lattice case. This is because there are no more points of the frame in the middle and the final configuration can return close to the initial.

7 Conclusions

In this work, we have presented some numerical simulations regarding strain deformation of a continuum medium. We started from an initial configuration imposed a strain and calculated the deformed configuration, using a position-based dynamics method able to take in account complex physical effects. This means that deformation configuration is calculated not by Newton law but only by the relative positions between the particles of the system and the characteristics of the lattice. In a preceding work, we verified the results of this tool are in accordance with results obtained by FEM, also in the fracture case; so far, in this paper, we have tried to generalize its application. We have showed a computational tool able to describe the behaviour of different materials, by changing some parameters of the algorithm. Computational costs are low because we do not solve differential equations but only algebraic equation systems. Working with a transformation operator between matrices the job can be parallelized between the GPU cores of the powerful video card. This is not a new kind of physics, just a graphic representation of a plausible behaviour; keep in mind that, up to now, you do not start from the constitutive equations of the materials leading to the rules governing points displacement. Actually, we just imitate a known behaviour adjusting the algorithm parameters. Anyway, the results are also interesting even if still in a preliminary form; in a next paper, we shall try to connect the rules of our model with physical proprieties of the material. Pseudoenergetic considerations are introduced to describe different deformation regimes, such as elastic and plastic and to achieve a better understanding of the process. This is preliminary to introducing potential descriptive interactions depending on the relative distance between the particles, which are able to reproduce the well known physical behaviour. Many questions remain open. How stable and robust is the model? What is possible to reasonably describe with this model and what are the physical reasons of its success? Is there a hidden dynamic? Does a connection exist between pseudoenergy and a real potential?

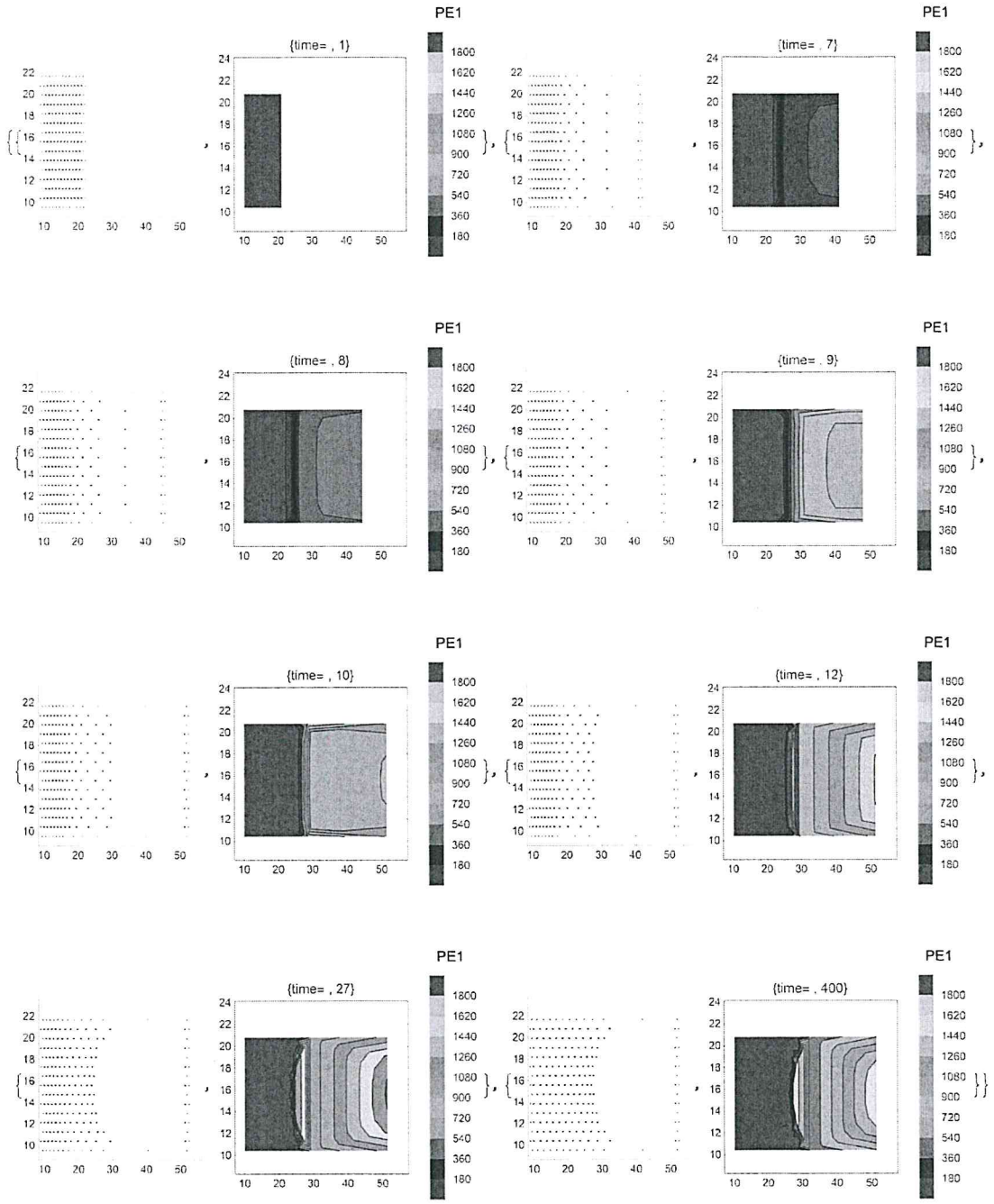

Fig. 18 Configuration of the lattice over different time (1, 7, 8, 9, 10, 12, 27 and 400) and PE1 contour plot

Does a physical meaning exist (like Hooke's law) of the position rules? How are the constitutive equations linked to the mixed interaction position rules, used to describe the Poisson effect? What kind of rules do we need for oscillation? Finally, the mathematical study of the homogenization of lattice systems like the one here considered seems to pose interesting problems and will probably require non-trivial ideas in the field of functional convergence [59–64]. These, and many others, are the object of a next paper, together with a

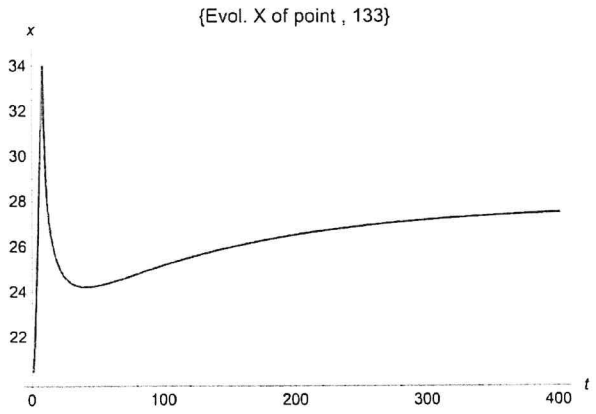

Fig. 19 Evolution of the central point $j = 133$ versus time

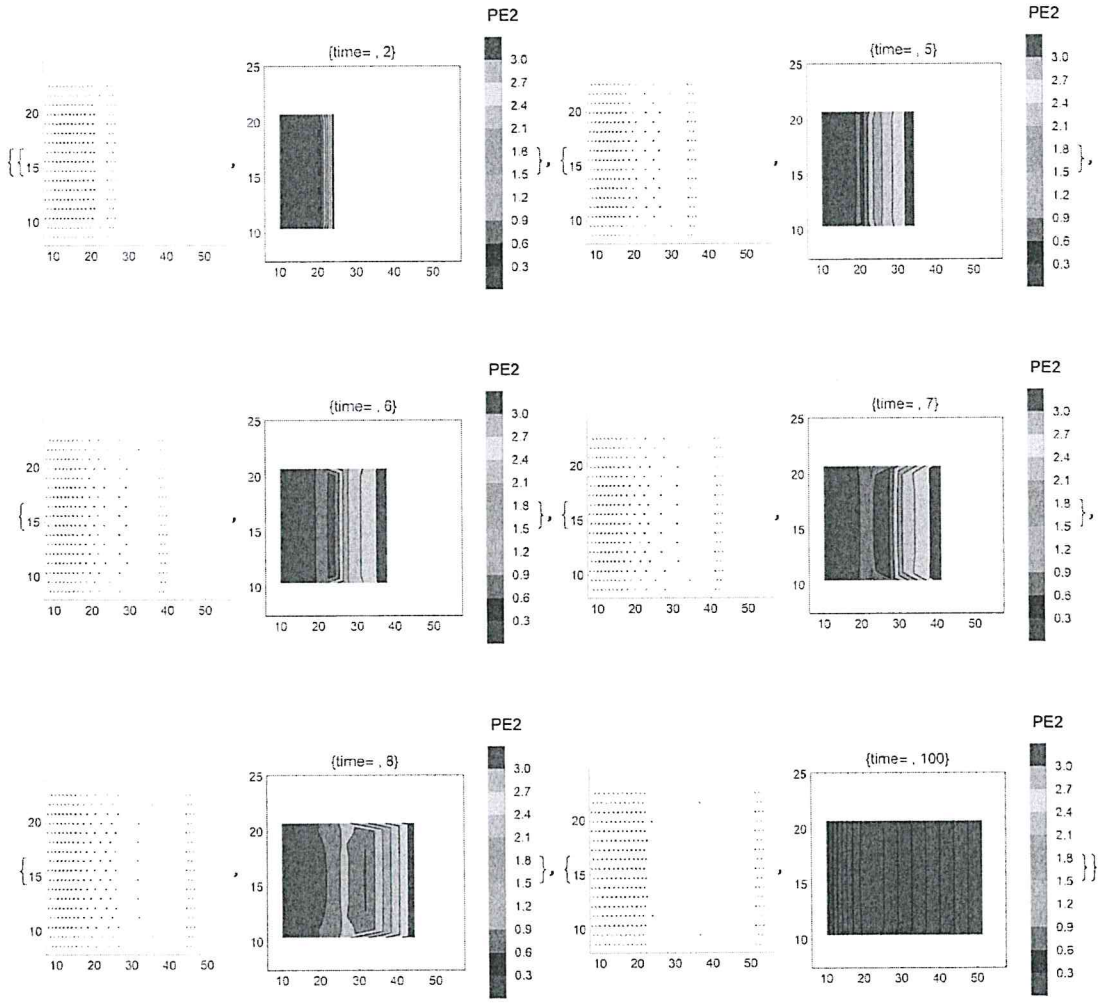

Fig. 20 Configuration of the lattice over different time (1, 7, 8, 9, 10, 12, 27 and 401) and PE1 contour plot

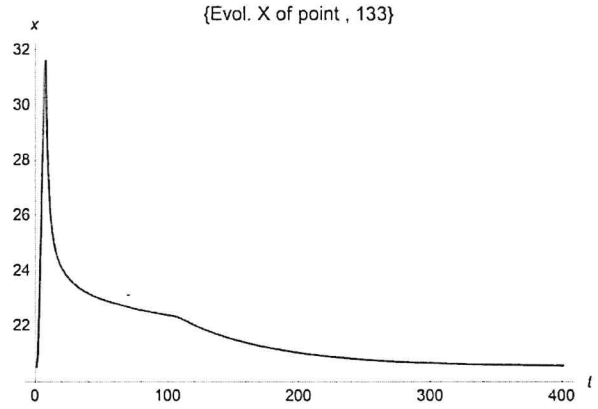

Fig. 21 Evolution of the central point $j = 133$ versus time

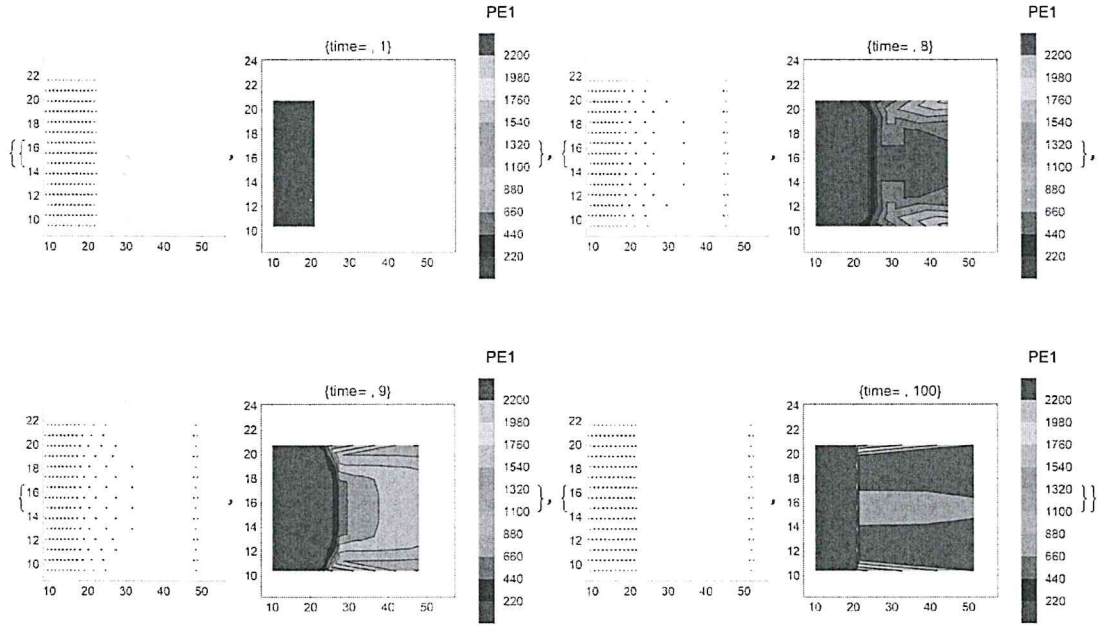

Fig. 22 Configuration of the lattice for different time (1, 8, 9 and 100) and PE1 contour plot

generalization in 3D. In order to meet the richness of behaviour of different materials, including potentially complex biological tissues [65–70], some other interesting behaviours are under study.

References

1. Bender, J., Müller, M., Macklin, M.: Position-based simulation methods in computer graphics. In: Eurographics 2015 Tutorials, Eurographics Association, Zurich, Switzerland (2015)
2. Bender, J., Koschier, D., Charrier, P., Weber, D.: Position-based simulation of continuous materials. Comput. Graph. **44**, 1–10 (2014)
3. Rivers, A.R., James, D.: FastLSM: fast lattice shape matching for robust real-time deformation. ACM Trans. Graph. **26**, 82 (2007). https://doi.org/10.1145/1275808.1276480
4. Diziol, R., Bender, J., Bayer, D.: Robust real-time deformation of incompressible surface meshes. In: Proceedings of the 2011 ACM SIGGRAPH/Eurographics Symposium on Computer Animation, New York, NY, USA, pp. 237–246 (2011)

5. Macklin, M., Müller, M., Chentanez, N.: XPBD: position-based simulation of compliant constrained dynamics. In: Proceeding MIG '16 Proceedings of the 9th International Conference on Motion in Games, pp. 49–54 (2016). https://doi.org/10.1145/2994258.2994272
6. Battista, A., Rosa, L., dell'Erba, R., Greco, L.: Numerical investigation of a particle system compared with first and second gradient continua: deformation and fracture phenomena*. Math. Mech. Solids, p. 1081286516657889, lug (2016)
7. Della Corte, A., Battista, A., dell'Isola, F.: Referential description of the evolution of a 2D swarm of robots interacting with the closer neighbors: perspectives of continuum modeling via higher gradient continua. Int. J. Non Linear Mech. **80**, 209–220 (2016)
8. Della Corte, A., Battista, A., dell'Isola, F., Giorgio, I.: Modeling deformable bodies using discrete systems with centroid-based propagating interaction: fracture and crack evolution. Mathematical Modelling in Solid Mechanics Volume 69 of the series Advanced Structured Materials, pp. 59–88 (2017)
9. Ern, A., Guermond, J.L.: Theory and Practice of Finite Elements, vol. 159. Springer, Berlin (2013)
10. Greco, L., Cuomo, M.: B-spline interpolation of Kirchhoff–Love space rods. Comput. Methods Appl. Mech. Eng. **256**, 251–269 (2013)
11. Greco, L., Cuomo, M.: An implicit G1 multi patch B-spline interpolation for Kirchhoff–Love space rod. Comput. Methods Appl. Mech. Eng. **269**, 173–197 (2014)
12. Contrafatto, L., Cuomo, M., Fazio, F.: An enriched finite element for crack opening and rebar slip in reinforced concrete members. Int. J. Fract. **178**, 33–50 (2012)
13. dell'Isola, F., Giorgio, I., Andreaus, U.: Elastic pantographic 2D lattices: a numerical analysis on the static response and wave propagation. Proc. Est. Acad. Sci. **64**(3), 219 (2015)
14. Cazzani, A., Malagù, M., Turco, E.: Isogeometric analysis of plane-curved beams. Math. Mech. Solids **21**(5), 562–577 (2016)
15. Cazzani, A., Stochino, F., Turco, E.: An analytical assessment of finite element and isogeometric analyses of the whole spectrum of Timoshenko beams. ZAMM J. Appl. Math. Mech. **96**(10), 1220–1244 (2016)
16. Bilotta, A., Turco, E.: A numerical study on the solution of the Cauchy problem in elasticity. Int. J. Solids Struct. **46**(25), 4451–4477 (2009)
17. Placidi, L., Greve, R., Seddik, H., Faria, S.H.: Continuum-mechanical, anisotropic flow model for polar ice masses, based on an anisotropic flow enhancement factor. Continuum Mech. Thermodyn. **22**(3), 221–237 (2010)
18. Placidi, L., Giorgio, I., Della Corte, A., Scerrato, D.: Euromech 563 Cisterna di Latina 17–21 March 2014 generalized continua and their applications to the design of composites and metamaterials: a review of presentations and discussions. Math. Mech. Solids **22**(2), 144–157 (2017)
19. Dell'Isola, F., Steigmann, D., Della Corte, A.: Synthesis of fibrous complex structures: designing microstructure to deliver targeted macroscale response. Appl. Mech. Rev. **67**(6), 060804 (2016)
20. Altenbach, J., Altenbach, H., Eremeyev, V.A.: On generalized Cosserat-type theories of plates and shells: a short review and bibliography. Arch. Appl. Mech. **80**(1), 73–92 (2010)
21. Altenbach, H., Eremeyev, V.A.: On the linear theory of micropolar plates. ZAMM J. Appl. Math. Mech. **89**(4), 242–256 (2009)
22. Eremeyev, V.A., Lebedev, L.P., Altenbach, H.: Foundations of Micropolar Mechanics. Springer, Berlin (2012)
23. Altenbach, H., Eremeyev, V.A.: Cosserat-type shells. In Generalized continua from the theory to engineering applications. Springer, Vienna, pp. 131–178 (2013)
24. Altenbach, H., Eremeyev, V.A. (eds.): Generalized Continua-from the Theory to Engineering Applications, vol. 541. Springer, Berlin (2012)
25. Altenbach, H., Bîrsan, M., Eremeyev, V.A.: Cosserat-type rods. In: Altenbach, H., Eremeyev, V.A. (eds.) Generalized Continua from the Theory to Engineering Applications. CISM International Centre for Mechanical Sciences (Courses and Lectures), vol. 541, pp. 179–248. Springer, Vienna (2013)
26. Eremeyev, V.A., Pietraszkiewicz, W.: Material symmetry group and constitutive equations of anisotropic Cosserat continuum. Gen. Contin. Models Mater. 10 (2012)
27. Eremeyev, V.A., Pietraszkiewicz, W.: Material symmetry group of the non-linear polar-elastic continuum. Int. J. Solids Struct. **49**(14), 1993–2005 (2012)
28. Forest, S.: Micromorphic approach for gradient elasticity, viscoplasticity, and damage. J. Eng. Mech. **135**(3), 117–131 (2009)
29. Abali, B.E., Müller, W.H., dell'Isola, F.: Theory and computation of higher gradient elasticity theories based on action principles. Arch. Appl. Mech. **05**, 1–16 (2017)
30. Cuomo, M., dell'Isola, F., Greco, L., Rizzi, N.L.: First versus second gradient energies for planar sheets with two families of inextensible fibres: investigation on deformation boundary layers, discontinuities and geometrical instabilities. Compos. B Eng. **115**, 423–448 (2017)
31. Turco, E., dell'Isola, F., Cazzani, A., Rizzi, N.L.: Hencky-type discrete model for pantographic structures: numerical comparison with second gradient continuum models. Zeitschrift für angewandte Mathematik und Physik **67**(4), 85 (2016)
32. dell'Isola, F., Madeo, A., Seppecher, P.: Cauchy tetrahedron argument applied to higher contact interactions. Arch. Ration. Mech. Anal. **219**(3), 1305–1341 (2016)
33. dell'Isola, F., Seppecher, P., Della Corte, A.: The postulations á la D'Alembert and á la Cauchy for higher gradient continuum theories are equivalent: a review of existing results. Proc. R. Soc. A **471**(2183), 20150415 (2015)
34. Javili, A., dell'Isola, F., Steinmann, P.: Geometrically nonlinear higher-gradient elasticity with energetic boundaries. J. Mech. Phys. Solids **61**, 21 (2013)
35. Alibert, J., Seppecher, P., dell'Isola, F.: Truss modular beams with deformation energy depending on higher displacement gradients. Math. Mech. Solids **8**(1), 51–73 (2003)
36. Forest, S., Cordero, N.M., Busso, E.P.: First vs. second gradient of strain theory for capillarity effects in an elastic fluid at small length scales. Comput. Mater. Sci. **50**(4), 1299–1304 (2011)

37. Placidi, L.: A variational approach for a nonlinear 1-dimensional second gradient continuum damage model. Contin. Mech. Thermodyn. **27**(4–5), 623 (2015)
38. Rosi, G., Giorgio, I., Eremeyev, V.A.: Propagation of linear compression waves through plane interfacial layers and mass adsorption in second gradient fluids. ZAMM J. Appl. Math. Mech. **93**(12), 914–927 (2013)
39. dell'Isola, F., Andreaus, U., Placidi, L.: At the origins and in the vanguard of peridynamics, non-local and higher gradient continuum mechanics. An underestimated and still topical contribution of Gabrio Piola. Mech. Math. Solids (MMS) **20**(8), 887–928. (Published online beforeprintFebruary 2, 2014) (2015)
40. Lanczos, C.: The Variational Principles of Mechanics. Courier Corporation, North Chelmsford (2012)
41. Placidi, L., dell'Isola, F., Ianiro, N., Sciarra, G.: Variational formulation of pre-stressed solid–fluid mixture theory, with an application to wave phenomena. Eur. J. Mech. A Solids **27**(4), 582–606 (2008)
42. dell'Isola, F., Placidi, L.: Variational principles are a powerful tool also for formulating field theories. In Variational Models and Methods in Solid and Fluid Mechanics. Springer, Vienna, pp. 1–15 (2011)
43. dell'Isola, F., Della Corte, A., Greco, L., Luongo, A.: Plane bias extension test for a continuum with two inextensible families of fibers: a variational treatment with Lagrange multipliers and a perturbation solution. Int. J. Solids Struct. **81**, 1–12 (2016)
44. dell'Isola, F., Gavrilyuk, S.L. (eds.): Variational Models and Methods in Solid and Fluid Mechanics, vol. 535. Springer, Berlin (2012)
45. dell'Isola, F., Auffray, N., Eremeyev, V.A., Madeo, A., Placidi, L., Rosi, G.: Least action principle for second gradient continua and capillary fluids: a Lagrangian approach following Piola's point of view. In The Complete Works of Gabrio Piola, vol. I, pp. 606–694. Springer (2014)
46. Ladevèze, P.: Nonlinear Computational Structural Mechanics: New Approaches and Non-incremental Methods of Calculation. Springer, Berlin (2012)
47. Steigmann, D.J.: Koiter's shell theory from the perspective of three-dimensional nonlinear elasticity. J. Elast. **111**(1), 91–107 (2013)
48. Steigmann, D.J.: A concise derivation of membrane theory from three-dimensional nonlinear elasticity. J. Elast. **97**(1), 97–101 (2009)
49. Steigmann, D.J.: Applications of polyconvexity and strong ellipticity to nonlinear elasticity and elastic plate theory. CISM Course Appl. Poly Quasi Rank One Convexity Appl. Mech. **516**, 265–299 (2010)
50. dell'Isola, F., Giorgio, I., Pawlikowski, M., Rizzi, N.L.: Large deformations of planar extensible beams and pantographic lattices: heuristic homogenization, experimental and numerical examples of equilibrium. Proc. R. Soc. A **472**(2185), 20150790 (2016)
51. Della Corte, A., dell'Isola, F., Esposito, R., Pulvirenti, M.: Equilibria of a clamped Euler beam (Elastica) with distributed load: large deformations. Math. Models Methods Appl. Sci. **27**(08), 1391–1421 (2017)
52. Gabriele, S., Rizzi, N.L., Varano, V.: A one-dimensional nonlinear thin walled beam model derived from Koiter shell theory. In: Topping, B.H.V., Iványi, P. (eds.) Proceedings of the Twelfth International Conference on Computational Structures Technology, Civil-Comp Press, Stirlingshire, UK, Paper 156 (2014). https://doi.org/10.4203/ccp.106.156
53. dell'Erba, R.: Determination of spatial configuration of an underwater swarm with minimum data. Int. J. Adv. Robot. Syst. **12**, 97 (2015)
54. Moriconi, C., dell'Erba, R.: The localization problem for harness: a multipurpose robotic swarm. In: SENSORCOMM 2012, The Sixth International Conference on Sensor Technologies and Applications, pp. 327–333 (2012)
55. Karaboga, D.: An idea based on honey bee swarm for numerical optimization. Technical report-tr06, Erciyes University, Engineering Faculty, Computer Engineering Department (2005)
56. Passino, K.M., Seeley, T.D., Visscher, P.K.: Swarm cognition in honey bees. Behav. Ecol. Sociobiol. **62**(3), 401–414 (2007)
57. Janson, S., Middendorf, M., Beekman, M.: Honeybee swarms: how do scouts guide a swarm of uninformed bees? Anim. Behav. **70**(2), 349–358 (2005)
58. Khatib, O., Kumar, V., Rus, D.: Experimental Robotics: The 10th International Symposium on Experimental Robotics. Springer, Berlin (2008)
59. Dos Reis, F., Ganghoffer, J.F.: Equivalent mechanical properties of auxetic lattices from discrete homogenization. Comput. Mater. Sci. **51**(1), 314–321 (2012)
60. Dos Reis, F., Ganghoffer, J.F.: Construction of micropolar continua from the asymptotic homogenization of beam lattices. Comput. Struct. **112**, 354–363 (2012)
61. Rahali, Y., Giorgio, I., Ganghoffer, J.F., dell'Isola, F.: Homogenization à la Piola produces second gradient continuum models for linear pantographic lattices. Int. J. Eng. Sci. **97**, 148–172 (2015)
62. Goda, I., Assidi, M., Ganghoffer, J.F.: Equivalent mechanical properties of textile monolayers from discrete asymptotic homogenization. J. Mech. Phys. Solids **61**(12), 2537–2565 (2013)
63. Alibert, J.J., Della Corte, A., Giorgio, I., Battista, A.: Extensional Elastica in large deformation as\Gamma-limit of a discrete 1D mechanical system. Zeitschrift für angewandte Mathematik und Physik **68**(2), 42 (2017)
64. Alibert, J.J., Della Corte, A.: Second-gradient continua as homogenized limit of pantographic microstructured plates: a rigorous proof. Zeitschrift für angewandte Mathematik und Physik **66**(5), 2855–2870 (2015)
65. Keaveny, T.M., Morgan, E.F., Yeh, O.C.: Bone Mechanics. Biomedical Engineering and Design Handbook, pp. 221–243. McGraw-Hill, New York (2009)
66. Andreaus, U., Giorgio, I., Lekszycki, T.: A 2-D continuum model of a mixture of bone tissue and bio-resorbable material for simulating mass density redistribution under load slowly variable in time. ZAMM J. Appl. Math. Mech. **94**(12), 978–1000 (2014)
67. Andreaus, U., Colloca, M., Iacoviello, D.: An optimal control procedure for bone adaptation under mechanical stimulus. Control Eng. Pract. **20**(6), 575–583 (2012)
68. Andreaus, U., Colloca, M., Toscano, A.: Mechanical behaviour of a prosthesized human femur: a comparative analysis between walking and stair climbing by using the finite element method. Biophys. Bioeng. Lett. **1**(3), 1–15 (2008)

69. Lekszycki, T., dell'Isola, F.: A mixture model with evolving mass densities for describing synthesis and resorption phenomena in bones reconstructed with bio-resorbable materials. ZAMM J. Appl. Math. Mech. **92**(6), 426–444 (2012)
70. Giorgio, I., Andreaus, U., Scerrato, D., dell'Isola, F.: A visco-poroelastic model of functional adaptation in bones reconstructed with bio-resorbable materials. Biomech. Model. Mechanobiol. **15**(5), 1325–1343 (2016)